Violation of Bell's inequality with continuous spatial variables

Ayman F. Abouraddy,[1,*] Timothy Yarnall,[2] Bahaa E. A. Saleh,[2] and Malvin C. Teich[2]
[1]*Research Laboratory of Electronics, Massachusetts Institute of Technology, Cambridge, Massachusetts 02139-4307, USA*
[2]*Quantum Imaging Laboratory, Departments of Electrical & Computer Engineering and Physics, Boston University, Boston, Massachusetts 02215-2421, USA*
(Received 5 October 2006; published 30 May 2007)

The Einstein-Podolsky-Rosen (EPR) argument revealed the paradoxical properties of a two-particle system entangled continuously in the spatial parameter. Yet a direct test of quantum nonlocality exhibited by this state, via a violation of Bell's inequality, has not been forthcoming. In this paper, we identify and construct experimental arrangements comprising simple optical components, without nonlinearities or moving parts, that implement operators in the spatial-parity space of single-photon fields that correspond to the familiar Pauli spin operators. We achieve this by first establishing an isomorphism between the *single-mode multiphoton* electromagnetic-field space spanned by a Fock-state basis and the *single-photon multimode* electromagnetic-field space spanned by a spatial-eigenmode basis. We then proceed to construct a Hilbert space with a two-dimensional basis of spatial even-odd parity modes. In particular, we describe an arrangement that implements a rotation in the parity space of each photon of an entangled-photon pair, allowing for a straightforward experimental test of Bell's inequality using the EPR state. Finally, the violation of a Bell inequality is quantified in terms of the physical parameters of the two-photon source.

DOI: 10.1103/PhysRevA.75.052114 PACS number(s): 03.65.Ud, 42.65.Lm, 03.67.Mn

I. INTRODUCTION

Seventy years ago, Einstein, Podolsky, and Rosen (EPR) [1] challenged the completeness of quantum mechanics by highlighting the correlations exhibited by two-particle systems described by the entangled EPR state

$$|\Psi\rangle = \int\int dx dx' \psi(x,x') |1_x, 1_{x'}\rangle, \tag{1}$$

with the un-normalized state function $\psi(x,x')=\delta(x-x')$; here $|1_x\rangle$ represents the one-dimensional (1D) position representation of a one-particle state. If the particles propagate freely, then measuring the particle positions reveals that they are always correlated, while momentum measurements reveal that they are anticorrelated, in apparent contradiction with the uncertainty principle [1,2]. However, most investigations of the EPR argument relied on the *discrete* Hilbert space of two entangled spin-$\frac{1}{2}$ particles suggested by Bohm (EPRB) [3], an example of which is

$$|\Psi\rangle = \frac{1}{\sqrt{2}}\{|\uparrow\uparrow\rangle + |\downarrow\downarrow\rangle\}. \tag{2}$$

In a typical scenario, each particle is subjected to a Stern-Gerlach device at angles θ_1 and θ_2, respectively. The spins are aligned when $\theta_1=\theta_2=0$ and antialigned when $\theta_1=-\theta_2=\frac{\pi}{2}$, in analogy to the position and momentum measurements in the EPR scheme, respectively.

Bell's celebrated inequality showed that quantum *nonlocality* is exhibited by the EPRB state when *intermediate* angle settings are probed [4], a feature not captured by the original EPR argument. In the Clauser-Horne-Shimony-Holt (CHSH) embodiment of Bell's inequality [5], local reality implies that

$$\mathcal{B} = E_s(\theta_1,\theta_2) + E_s(\theta_1,\theta_2') + E_s(\theta_1',\theta_2) - E_s(\theta_1',\theta_2') \leqslant 2, \tag{3}$$

where E_s ($|E_s|\leqslant 1$) is the expected value of the correlation between the two spin directions (i.e., the statistical correlation between the counting rates in two counters in one arm of the apparatus and those in the other arm). The CHSH inequality is violated by the EPRB state in Eq. (2) where $E_s(\theta_1,\theta_2)=\cos(\theta_1-\theta_2)$ and $\mathcal{B}$ reaches a maximum value of $2\sqrt{2}$ (the C'irelson limit) when $\theta_1=-\theta_2=\frac{\pi}{8}$ and $\theta_1'=-\theta_2'=\frac{13\pi}{8}$, for example. The violation of Bell's inequality using the EPRB state has been firmly established in numerous experiments [6–12], which have led to the development of applications such as quantum cryptography [13–15] and quantum teleportation [16–18], among others, thereby fueling interest in the burgeoning domain of quantum information [19]. The EPRB state has become a cornerstone of experimental quantum information science since it is readily produced by the process of optical spontaneous parametric downconversion (SPDC) in polarization space [20–22], following appropriate filtering of the spatial and spectral degrees of freedom, or, equivalently, in the discrete spatial domain [10] or in the time-energy domain [23–25].

Nevertheless, interest in continuous quantum variables, such as those of the EPR state, has persisted, although the communities that study discrete and continuous variables tend to be distinct (see Ref. [26] for a recent survey of the continuous quantum variables literature). One aspect of the problem is the identification of canonical continuous quantum variables, corresponding to the position and momentum variables discussed by EPR, that are easily accessed experimentally. An approach to testing the predictions of the original EPR argument using continuous quantum variables was proposed by Reid and Drummond in 1988 [27] where measurements of the quadratures of the signal and idler optical fields produced by a nondegenerate parametric oscillator

*Email address: raddy@mit.edu

above threshold replace the position and momentum measurements. Their proposal was later verified experimentally by Ou *et al.* [28]. More recently, the EPR proposal was demonstrated experimentally by Howell *et al.* [29], where the position and momentum measurements were performed by measuring the near- and far-field diffraction patterns of SPDC obtained by different placements of lenses in the path of the signal and idler photons and an inequality involving the products of the widths of patterns showed an apparent violation of the uncertainty principle.

While these experiments indeed verify the EPR paradox, they do not constitute a test of quantum nonlocality via a violation of Bell's inequality. In fact, Bell argued that the EPR state would not violate the CHSH inequality, and thus does not exhibit quantum nonlocality [30]. His argument is based on the observation that the Wigner distribution [31] associated with the EPR state is non-negative everywhere, and thus admits a local and realistic hidden-variables model. This statement has spurred many investigations that have critiqued Bell's argument and shown it to be erroneous by proposing counterexamples in which an EPR state is predicted to yield a violation of Bell's inequality [32–36]. Several proposed experimental arrangements for testing quantum nonlocality of the EPR state were subsequently considered [37–39]. While these schemes are feasible in principle, they nevertheless present considerable experimental difficulties. The approach suggested by Chen *et al.* [36], for example, describes the construction of abstract *pseudospin* operators (so named because of apparent similarity to the familiar Pauli spin-$\frac{1}{2}$ operators) defined in the Fock basis of a single-mode electromagnetic field. But the experimental realization of these pseudospin operators requires complex photon-atom interactions [36].

The theoretical underpinning for violating Bell's inequality with an EPR state was recently elucidated by Revzen *et al.* [40]. These authors demonstrate that the non-negativity of the Wigner distribution is not a *sufficient* condition for satisfying the CHSH inequality; rather, a further condition on the allowed *observables* is required. A class of observables that Revzen *et al.* term "nonproper" observables is associated with an evolution of the associated Wigner distribution, in the Schrödinger picture, into one that is not non-negative everywhere. It turns out that the pseudospin operators proposed by Chen *et al.* [36] fall into this class (as do all of the constructs that show a violation of Bell's inequality using the EPR state [34]). This is precisely the class that was overlooked by Bell.

In this paper, we complete the EPR-Bell program by showing that an entangled EPR state in the spatial domain violates a Bell inequality and hence demonstrates quantum nonlocality. Our proposal retains the original EPR state in the continuous spatial domain [Eq. (1)] while permitting a violation of the CHSH inequality that relies on dichotomic quantum variables. The 2D Hilbert space constructed for each photon is the parity space in the one-dimensional spatial domain, where parity refers to the even-odd modal content of the photon spatial profile.

We begin by constructing an isomorphism between the *single-mode multiphoton* electromagnetic-field space spanned by a Fock-state basis (such as that used by Chen *et al.* [36] to construct pseudospin operators) and the single-photon multimode electromagnetic-field space spanned by a spatial-eigenmode basis, and construct the parity space in this basis. We then proceed to describe a set of optical arrangements, suggested by this isomorphism, that implement relevant operators on parity space. The arrangements rely on simple linear optical components, and require no nonlinearities or moving parts. In particular, we describe a simple optical device that applies a rotation [an SO(2) operator] in parity space. This, in turn, allows us to construct an arrangement for testing the CHSH inequality by implementing two SO(2) operators, one for each photon of a two-photon source, here taken to be SPDC-produced entangled photon pairs. The extent of the violation of the CHSH inequality is quantified in terms of the physical parameters of the two-photon source, namely, the width of the pump spatial profile and the thickness of the nonlinear crystal. We complete the paper by comparing our proposal to other approaches and by outlining some future possibilities for this scheme.

For the sake of completeness, we mention other relevant work that makes use of the spatial degree of freedom of entangled photon pairs. Early work examined the spatial coherence of photon pairs produced by SPDC [41–45]. This led to the development of a paradigm usually known as quantum imaging [46–50], which explores the unusual imaging configurations offered by entangled photon pairs. More recently, efforts have been directed to studying discretized spatial domains [51,52], interference effects arising from the spatial profile of the SPDC pump, and orbital angular momentum. One well-studied and widely used two-photon interferometer is the Hong-Ou-Mandel interferometer [53]. While this is a temporal interferometer, the effect of the spatial parameter on the interferogram has attracted substantial attention [54–60]. The effect of the spatial pump profile on the spectrum of the entangled photons produced by SPDC has also been considered [61,62]. The work presented in this paper establishes a bridgehead between the overall research effort in quantum imaging and that of the mainstream quantum-information-processing community, which, by-and-large, relies on the spin-$\frac{1}{2}$ formalism.

II. STRATEGY FOR MANIPULATING CONTINUOUS SPATIAL VARIABLES IN PARITY SPACE

While the EPRB state and the associated CHSH inequality may be easily analyzed in terms of the Pauli spin-$\frac{1}{2}$ (or 2-level) operators $(\sigma_x, \sigma_y, \sigma_y)$, the situation is more involved if the particles inhabit Hilbert spaces of larger (potentially infinite) dimension. One approach to manage such a large-dimension Hilbert space is to map it onto a Hilbert space of lesser dimension. A general procedure for mapping a continuous-variable system onto a discrete one of arbitrary dimension has been outlined by Brukner *et al.* [63].

A particular instance of this mapping was detailed by Chen *et al.* [36], where a discretely infinite dimensional Hilbert space was mapped onto a 2D space. This mapping was accomplished by constructing a generalization of the Pauli operators for the case of a single-mode electromagnetic field in the Fock basis. These are the so-called *pseudospin* operators:

$$s_x = \sum_{n=0}^{\infty} (|2n+1\rangle\langle 2n| + |2n\rangle\langle 2n+1|),$$

$$s_y = i\sum_{n=0}^{\infty} (|2n+1\rangle\langle 2n| - |2n\rangle\langle 2n+1|),$$

$$s_z = \sum_{n=0}^{\infty} (|2n\rangle\langle 2n| - |2n+1\rangle\langle 2n+1|). \quad (4)$$

One may also define a "raising" operator $s^+ = \Sigma_n |2n+1\rangle\langle 2n|$ and a "lowering" operator $s^- = \Sigma_n |2n\rangle\langle 2n+1|$. The question of how to construct an experimental realization of pseudospin operators nevertheless remains challenging.

One of the principal results of this paper is to establish an isomorphism between the *single-mode multiphoton* electromagnetic-field space spanned by the Fock-state basis $\{|n\rangle\}$ (pseudospin space) and the *single-photon multimode* electromagnetic-field space spanned by a spatial-eigenmode basis $\{\phi_n(x)\}$ (which we henceforth call *parity* space). Our overall strategy is to identify each Fock state with a spatial mode, $|n\rangle \rightarrow |\phi_n\rangle$, which then enables us to construct parity-space operators in the spatial domain that are straightforward to implement.

We begin by considering a pure single-photon multimode state in the 1D spatial domain (in anticipation of the two-photon case where we use a 1D approximation as discussed in Appendix A) given in general by [47]

$$|\Psi\rangle = \int dx \psi(x) |1_x\rangle, \quad (5)$$

where $\int dx |\psi(x)|^2 = 1$. Here x refers the direction normal to the photon general direction of propagation. Any orthonormal basis over L_2 can be used to decompose the state function ψ,

$$\psi(x) = \sum_{n=0}^{\infty} c_n \phi_n(x), \quad (6)$$

where $\Sigma_n |c_n|^2 = 1$ and $c_n = \int dx \phi_n^*(x) \psi(x)$. The state may thereby be recast in the form

$$|\Psi\rangle = \sum_{n=0}^{\infty} c_n \int dx \phi_n(x) |1_x\rangle = \sum_{n=0}^{\infty} c_n |n\rangle, \quad (7)$$

where we have made the association $\int dx \phi_n(x) |1_x\rangle = |n\rangle$.

A convenient discrete basis for L_2 is (amongst others) the set of Hermite-Gaussian functions. A particular characteristic of this set of functions of interest to us is that their sequence alternates between even and odd functions, i.e., $\phi_{2n}(-x) = \phi_{2n}(x)$ and $\phi_{2n+1}(-x) = -\phi_{2n+1}(x)$, $\forall n$. Thus, an *algebraic* property of the sequence of integer numbers $\{n\}$, namely, the alternation of even and odd integers, is associated with a *functional* property of the sequence of functions $\{\phi_n(x)\}$, namely, the alternation of even- and odd-parity spatial modes. Given this association, one may decompose the state in Eq. (7) into even ($|\mathrm{e}\rangle$) and odd ($|\mathrm{o}\rangle$) spatial-parity components

$$|\Psi\rangle = \sum_{n=0}^{\infty} c_{2n} |2n\rangle + \sum_{n=0}^{\infty} c_{2n+1} |2n+1\rangle = \alpha |\mathrm{e}\rangle + \beta |\mathrm{o}\rangle, \quad (8)$$

where $\langle \mathrm{e}|\mathrm{e}\rangle = \langle \mathrm{o}|\mathrm{o}\rangle = 1$, $|\alpha|^2 = \Sigma_{2n} |c_{2n}|^2$, $|\beta|^2 = \Sigma_{2n+1} |c_{2n+1}|^2$, and $|\alpha|^2 + |\beta|^2 = 1$.

This procedure establishes three levels of description for the one-photon state: (1) the spatial-parameter description of Eq. (5); (2) the discretized spatial eigenmode description given by Eq. (7); and (3) the spatial-parity-space description provided by Eq. (8). In Appendix B we consider the spatial-parity *operators* S_x, S_y, and S_z in these three levels of description.

The advantage of our approach, in comparison with that based on the Fock basis for the single-mode multiphoton electromagnetic field, is that experimental realizations of the abstract spatial-parity operators (and others) are readily implemented in the spatial domain. Indeed, a wide range of relevant optical transformations developed in the optical-imaging community may be implemented in the spatial domain, as we demonstrate in the next section.

III. CONSTRUCTION OF OPERATORS IN ONE-PHOTON PARITY SPACE

In this section we describe the construction of a set of optical arrangements that implement operators on the parity space of a one-photon field in the 1D spatial domain. A common feature of these arrangements is their simplicity. In particular, no nonlinearities or moving parts (such as scanning elements) are required to implement any prescribed operator.

A. Parity flipper

The pseudospin operator $s^+ = \Sigma_{n=0} |2n+1\rangle\langle 2n|$ is particularly difficult to implement in the Fock basis since it requires adding a single photon to the input field if the number of existing photons is even, thus converting the number of photons from even to odd. However, in the spatial domain, where the Fock photon-number basis is identified with the order of a spatial eigenmode, a simple construction exists that readily achieves this operation. In the spatial domain, an optical system that transforms an odd mode to an even mode (and vice versa), which we term a parity flipper, is a simple phase plate that takes the form $h_{\mathrm{PF}}(x,x') = h(x)\delta(x-x')$, where $h(x) = e^{i\pi H(x)}$ and $H(x)$ is the Heaviside step function, $H(x) = 1$ for $x > 0$ and is otherwise equal to 0, shown symbolically in Fig. 1(a). In other words, half of the single-photon wave front passes with no change, while a phase π is imparted uniformly to the other half of the wave front. Note that no loss of photons is incurred by using such a phase plate.

For reasons that will become clear shortly, we express the parity flipper as $h(x) = -iR_\pi(x)$, where the phase plate $R_\pi(x)$ is characterized by $|R_\pi(x)| = 1$, $\forall x$, while $\angle R_\pi(x) = \frac{\pi}{2}$ for $x \geqslant 0$ and $\angle R_\pi(x) = -\frac{\pi}{2}$ for $x < 0$. Thus, except for an unimportant overall phase, the parity flipper is implemented with the phase plate $R_\pi(x)$. In Appendix C we define spaces that are *closed* under this parity-flip operation, where it corresponds exactly to the S_x spatial-parity operator.

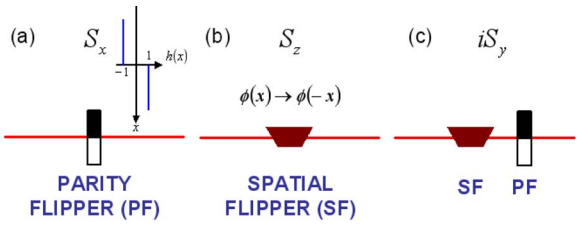

FIG. 1. (Color online) Schematics of optical arrangements in the spatial domain for one-photon spatial-parity operators. (a) A parity flipper (PF) introduces a π phase shift between the two halves of the input plane. The inset shows the transmittance $h(x)$ of the phase plate. For subspaces of L_2 closed under the parity flip (see text for details), this device corresponds to the operator S_x. (b) A spatial flipper (SF) implements the transformation $\phi(x) \to \phi(-x)$ in 1D, where $\phi(x)$ is the input field distribution. This device corresponds to the operator S_z. (c) A cascade of operators S_z from (b), followed by S_x from (a), corresponds to the operator iS_y.

B. Spatial flipper

Next we consider the spatial parity operator S_z that is implemented by an optical system whose impulse response function $h_z(x,x')$ is given in Eq. (B2) of Appendix B. The completeness of the basis set $\{\phi_n(x)\}$ implies that $\Sigma_{n=0}\phi_n(x)\phi_n^*(x') = \delta(x-x')$, and it is easy to then see that $h_z(x,x') = \delta(x+x')$. In other words, S_z corresponds to the transformation $\psi(x) \to \psi(-x)$ that may be readily implemented using mirrors, lenses, or other simple optical components. The effect of the spatial flipper (SF), shown symbolically in Fig. 1(b), is to flip an input optical field distribution about the origin, which is expressed mathematically in the three abovementioned levels of description as follows:

$$|\Psi\rangle \to \int dx \psi(-x)|1_x\rangle = \sum_{n=0}^{\infty} c_{2n}|2n\rangle - \sum_{n=0}^{\infty} c_{2n+1}|2n+1\rangle$$
$$= \alpha|\mathrm{e}\rangle - \beta|\mathrm{o}\rangle = S_z|\Psi\rangle. \quad (9)$$

Now that we have demonstrated how to construct the S_x (parity flipper in a subspace of L_2 closed under parity flip) and S_z (spatial flipper) operators, we can make use of the commutation relation $[S_z, S_x] = 2iS_y$ (or $S_zS_x = iS_y$) to construct the remaining parity operator S_y, as shown schematically in Fig. 1(c).

C. Parity analyzer

A parity analyzer (PA) is a device that separates a one-photon state into its even- and odd-parity spatial components. This corresponds to the operation of a polarizing beam splitter in polarization space or a Stern-Gerlach device in spin-$\frac{1}{2}$ space. Consider the arrangement displayed in Fig. 2(a) where a spatial flipper (SF) is inserted into one arm of a balanced Mach-Zehnder interferometer. This arrangement separates the input beam (at planes 0 or 1) into its odd and even components at the two output ports (planes 3 and 2). Both beam splitters are symmetric, with a transformation between the input and output ports that obeys $\frac{1}{\sqrt{2}}\begin{pmatrix} 1 & i \\ i & 1 \end{pmatrix}$. The super-operator transformation $\mathbf{P}$ between the input and output ports of this device may be expressed in matrix form as follows:

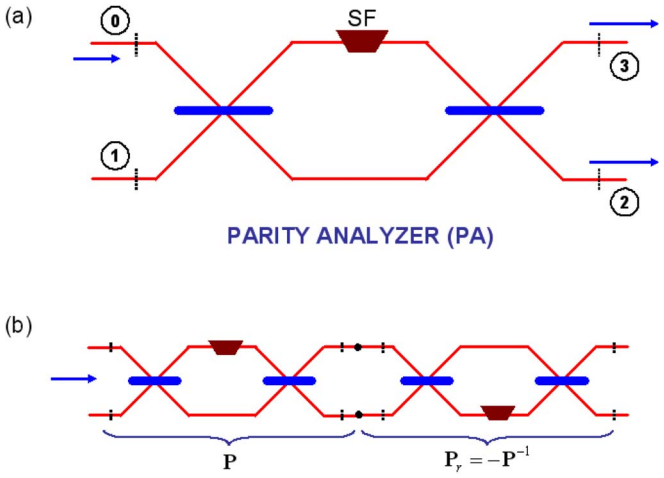

FIG. 2. (Color online) (a) Parity analyzer for a one-photon state. The device is a balanced Mach-Zehnder interferometer with a spatial flipper [SF, Fig. 1(b)] placed in one arm. This arrangement projects an arbitrary input state at plane 0 onto its odd and even components at planes 3 and 2, respectively. Alternatively, an arbitrary input state at plane 1 is projected onto its odd and even components at planes 2 and 3, respectively. (b) Cascade of a parity analyzer and an "inverse" parity analyzer.

$$\begin{pmatrix} \varphi_3(x) \\ \varphi_2(x) \end{pmatrix} = \underbrace{\begin{pmatrix} P_o & iP_e \\ iP_e & -P_o \end{pmatrix}}_{\mathbf{P}} \begin{pmatrix} \varphi_0(x) \\ \varphi_1(x) \end{pmatrix}. \quad (10)$$

The operators P_e and P_o are projection operators onto the even and odd spatial-parity subspaces, respectively, defined as

$$P_e = \frac{1}{2}\{\mathbb{I} + S_z\} = \sum_n |2n\rangle\langle 2n|,$$

$$P_o = \frac{1}{2}\{\mathbb{I} - S_z\} = \sum_n |2n+1\rangle\langle 2n+1|. \quad (11)$$

If the one-photon state is incident on port 0, the projections of the state onto the even and odd spatial parity subspaces emerge from ports 2 and 3, respectively. On the other hand, if the state is incident on port 1, the projections of the state onto the even and odd spatial parity subspaces emerge from ports 3 and 2, respectively.

Consider the arrangement illustrated in Fig. 2(b) where two cascaded parity analyzers are shown, but with the spatial flipper in the opposite arm of the second interferometer, and described with the transformation $\mathbf{P}_r$. The input-output transformation of this arrangement is

$$\mathbf{P}_r \cdot \mathbf{P} = -\begin{pmatrix} \mathbb{I} & 0 \\ 0 & \mathbb{I} \end{pmatrix}, \quad (12)$$

i.e., the parity analyzer with the relocated spatial flipper is the inverse of the parity analyzer in Fig. 2(a), with an unimportant overall phase $\mathbf{P}_r = -\mathbf{P}^{-1}$. Thus one may use a parity analyzer to first split an incoming one-photon state into its

even and odd spatial-parity projections and to separate them into two distinct spatial paths, to then manipulate the two components separately (without changing their parity), and finally to recombine them into a single spatial path using the "inverse" parity analyzer.

D. General SU(2) operator in parity space

To implement a Bell-inequality test on the parity space of two-photons, we need to construct SO(2) operators, and, more generally, SU(2) operators, on the one-photon parity space. One approach toward constructing a general SU(2) operator $\mathbf{U}_2$,

$$\mathbf{U}_2(\theta,\alpha,\beta)=\begin{pmatrix}\cos\frac{\theta}{2}e^{i\alpha} & i\sin\frac{\theta}{2}e^{i\beta}\\ i\sin\frac{\theta}{2}e^{-i\beta} & \cos\frac{\theta}{2}e^{-i\alpha}\end{pmatrix}, \tag{13}$$

makes use of the decomposition of the SU(2) operator in spin-$\frac{1}{2}$ space into a linear superposition of the Pauli spin (or spatial-parity) operators

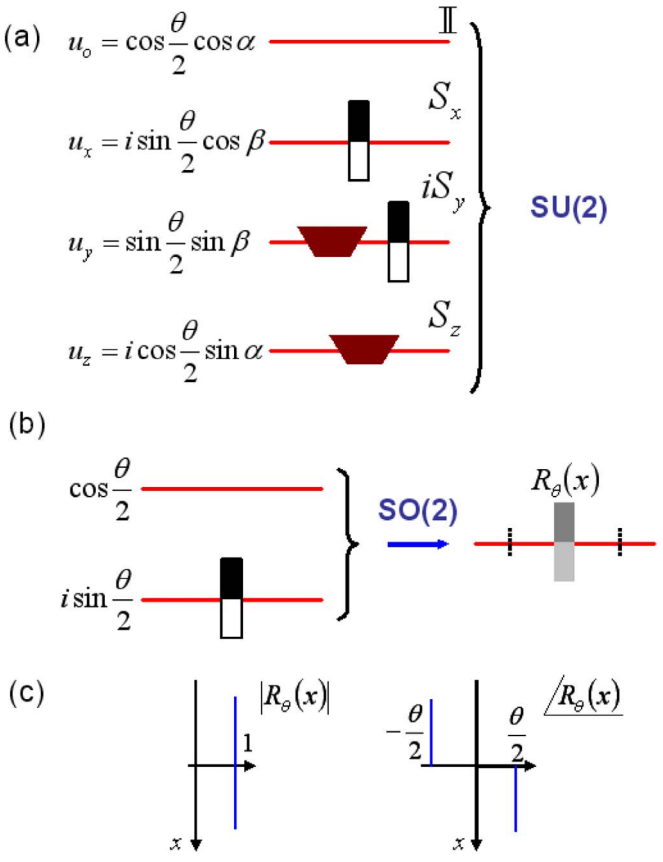

FIG. 3. (Color online) First approach to the construction of an SU(2) operator in parity space. (a) An SU(2) operator as a weighted superposition of the spatial parity operators [Eq. (14)]. (b) An SO(2) operator as a weighted superposition of the $\mathbb{I}$ and S_x parity operators. The right panel shows a phase plate $R_\theta(x)$ that performs the same task as that of the superposition on the left. (c) The amplitude transmittance and phase distribution of the phase plate $R_\theta(x)$ is shown in 1D.

$$\mathbf{U}_2=u_o\mathbb{I}+u_xS_x+u_yS_y+u_zS_z, \tag{14}$$

where $u_i=\frac{1}{2}\mathrm{Tr}\{S_i\mathbf{U}_2\}$, $i=o, x, y, z$, as shown schematically in Fig. 3(a). We consider explicitly the case of an SO(2) rotation operator

$$\mathbf{R}(\theta)=\begin{pmatrix}\cos\frac{\theta}{2} & i\sin\frac{\theta}{2}\\ i\sin\frac{\theta}{2} & \cos\frac{\theta}{2}\end{pmatrix}=\cos\frac{\theta}{2}\mathbb{I}+i\sin\frac{\theta}{2}S_x, \tag{15}$$

shown schematically in Fig. 3(b). The effect of this operator is to rotate the state by an angle θ in parity space. The optical system corresponding to this operator has the impulse response function

$$h_\theta(x,x')=\cos\frac{\theta}{2}h_1(x,x')+i\sin\frac{\theta}{2}h_x(x,x'),$$

$$=R_\theta(x)\delta(x-x'), \tag{16}$$

where $R_\theta(x)=\cos\frac{\theta}{2}+\sin\frac{\theta}{2}R_\pi(x)$. Thus, the rotation operator $\mathbf{R}(\theta)$ in *parity space* is implemented in the *spatial domain* using a phase plate having unity amplitude transmittance $|R_\theta(x)|=1$, $\forall x$ and $\forall\theta$, while imparting a phase $\angle R_\theta(x)=\frac{\theta}{2}$ for $x\geq 0$ and $\angle R_\theta(x)=-\frac{\theta}{2}$ for $x<0$, as schematized in Fig. 3(c). Such a transformation is readily attained by using spatial light modulators, which allow spatially varying phase distributions to be imparted to an optical wave front.

The second approach toward constructing a general SU(2) operator in parity space makes use of its factorization into a cascade of simpler operators

$$\mathbf{U}_2(\theta,\alpha,\beta)=\underbrace{\begin{pmatrix}e^{i(\alpha+\beta)/2} & 0\\ 0 & e^{-i(\alpha+\beta)/2}\end{pmatrix}}_{\mathrm{U}(1)}\underbrace{\begin{pmatrix}\cos\frac{\theta}{2} & i\sin\frac{\theta}{2}\\ i\sin\frac{\theta}{2} & \cos\frac{\theta}{2}\end{pmatrix}}_{\mathrm{SO}(2)}\times\underbrace{\begin{pmatrix}e^{i(\alpha-\beta)/2} & 0\\ 0 & e^{-i(\alpha-\beta)/2}\end{pmatrix}}_{\mathrm{U}(1)}, \tag{17}$$

each of which is easily implemented in the spatial domain. The U(1) transformation is simply a phase shift inserted in the even and odd components separated into two distinct paths at the output of a parity analyzer [Fig. 4(a)], whereas the SO(2) transformation is a beam splitter with variable reflectance (VBS) that mixes the even- and odd-parity components [Fig. 4(b)]. The arrangement in Fig. 4(c) shows an implementation of a general SU(2) operator in parity space in light of the decomposition offered by Eq. (17). The even and odd components may then be recombined using an "inverse" parity analyzer. Note that one may use the above-described construction of a general SU(2) operator to obtain a complete characterization of the one-photon state (whether pure or mixed) in parity space via quantum-state tomogra-

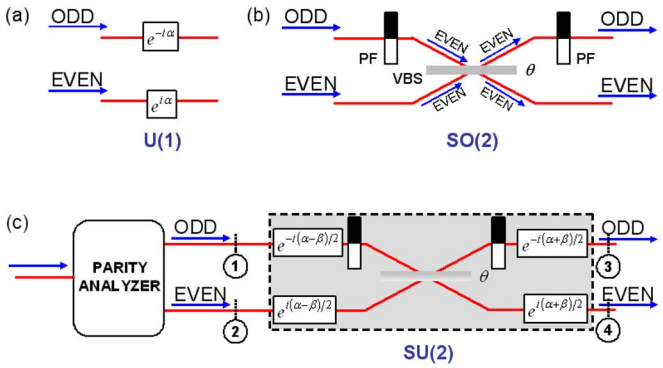

FIG. 4. (Color online) Second approach to the construction of an SU(2) operator in parity space as a cascade of simpler operations [Eq. (17)]. (a) A U(1) operator applies phases α and $-\alpha$ to the even and odd components, respectively. (b) An SO(2) operator mixes the even and odd modes at a beam splitter with variable reflectance (VBS). Since the even and odd modes are orthogonal, however, simply mixing them at a beam splitter will not produce the desired SO(2) operator; we must first convert the odd component to even using a PF. Both output components of the beam splitter then have even parity, and one is reverted back to odd parity using a PF. (c) The SU(2) operator, following a parity analyzer, is composed of an SO(2) operator as in (b), preceded and followed by two U(1) operators as in (a), implementing the appropriate phases as provided in Eq. (17).

phy, which requires implementing projection operators in rotated bases [64–67].

IV. TWO-PHOTON PARITY-SPACE ANALYZER

The isomorphism between the single-mode multiphoton electromagnetic-field space spanned by a Fock-state basis and the single-photon multimode electromagnetic-field space spanned by a spatial-eigenmode basis can be extended to two-photon states. We begin by writing the two-photon state function $\psi(x,x')$ [Eq. (1)] in terms of a discretized sum of eigenfunctions known as the Schmidt decomposition

$$\psi(x,x') = \sum_{n=0}^{\infty} \lambda_n \varphi_n(x) \xi_n(x'), \tag{18}$$

where $\Sigma_n |\lambda_n|^2 = 1$, and both $\{\varphi_n(x)\}$ and $\{\xi_n(x)\}$ are orthonormal bases for L_2. Note that no loss of generality is associated with the discretization, and the expansion is exact if all terms are retained [68–71]. A factorizable two-photon state is represented by a Schmidt decomposition with only one product term, whereas entangled states include more than one. We will focus on two classes of state functions, classified according to their symmetry under inversion through the origin of the $x-x'$ plane. The first class consists of state functions that behaves as $\psi(x,x') = \psi(-x,-x')$ (i.e., invariant under the inversion), while the second class behaves as $\psi(x,x') = -\psi(-x,-x')$. The practical importance of these two particular classes of two-photon states stems from the fact that they correspond to the state produced by SPDC when the spatial profile of the optical pump is even and odd, respectively, as

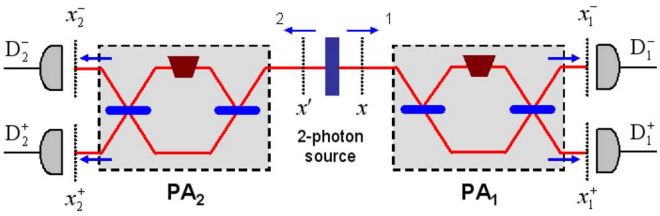

FIG. 5. (Color online) Parity projection for a two-photon source (2PS). Each photon (planes x and x') is directed into a parity analyzer PA_1 and PA_2). The even (plane x_1^+) and odd (plane x_1^-) components of photon 1 are detected by D_1^+ and D_1^-; similarly for photon 2. Each detector integrates over its plane, and all detectors for the two photons are connected to coincidence circuits.

described in Appendix A, and are thus readily achievable in practice. Note that we use the variables x and x' to refer to the source plane and the variables x_1 and x_2 to refer to the detector plane.

We consider first two-photon states having $\psi(x,x') = \psi(-x,-x')$ [and thus also $\psi(-x,x') = \psi(x,-x')$], the two-photon state produced by SPDC using an even pump. The condition $\psi(x,x') = \psi(-x,-x')$ implies two things: (1) the bases functions $\{\varphi_n(x)\}$ and $\{\xi_n(x)\}$ have *specific parity*, i.e., each function is *either* even *or* odd; and (2) the sequences of functions in the two bases are such that the corresponding functions $\varphi_n(x)$ and $\xi_n(x)$ in each term of the Schmidt decomposition [Eq. (18)] are *both even or both odd*, for all n. In particular, the maximally entangled EPR state with the ideal state function $\psi(x,x') = \delta(x-x')$ has the Schmidt decomposition

$$\psi(x,x') = \delta(x-x') = \sum_{n=0}^{\infty} \phi_n(x) \phi_n(x'), \tag{19}$$

where $\{\phi_n(x)\}$ are the Hermite-Gaussian functions, and all the coefficients in the Schmidt decomposition are equal.

The second class of two-photon states that we consider are those characterized by state functions having the property $\psi(x,x') = -\psi(-x,-x')$, which is produced with SPDC when the pump has an odd spatial profile. It is easy to see that this property also implies that the bases functions $\{\varphi_n(x)\}$ and $\{\xi_n(x)\}$ have specific parity (i.e., each function in both bases is either even or odd), but in this case the basis-function sequences are such that $\varphi_n(x)$ and $\xi_n(x)$ have opposite parities [i.e., when $\varphi_n(x)$ is even, then $\xi_n(x)$ is odd, and vice versa].

In light of the above classification, we now describe the effect of implementing two parity analyzers, one in the path of each photon from a pair of photons emitted by a two-photon source (2PS), which will help set the stage for our proposed experiment for violating Bell's inequality in the spatial domain. Each photon is guided to a separate parity analyzer as shown in Fig. 5. In this conception, a detector is placed at each exit port of both parity analyzers, the detectors integrate the arrival of photons over their respective planes, and singles and coincidence rates are recorded. The spatial coordinates at the exits of the even and odd ports of each PA are distinguished by superscripts "+" and "−," respectively.

Thus the output planes for photon 1 (traveling to the right in Fig. 5) are described by the spatial coordinates x_1^+ and x_1^-, and those for photon 2 (traveling to the left in Fig. 5) are x_2^+ and x_2^-. The detectors that detect the arrival of a photon over the plane are denoted in a similar manner; thus D_1^+ detects the arrival of a photon in the x_1^+ plane, and similarly for detectors D_1^-, D_2^+, and D_2^-.

The rate of coincidence of photon pairs at two points in the four pairs of planes $G(x_1^+,x_2^+)$, $G(x_1^+,x_2^-)$, $G(x_1^-,x_2^+)$, and $G(x_1^-,x_2^-)$, may be calculated by making use of the formalism developed by Saleh *et al.* [46]; the total coincidence rates of between each pair of detectors are obtained by integrating over the spatial variables

$$P(+,+) = \int\int dx_1^+ dx_2^+ G(x_1^+,x_2^+), \tag{20}$$

where $P(+,+)$ is the total coincidence rate between detectors D_1^+ and D_2^+, and similarly for the other total coincidence rates $P(+,-)$, $P(-,+)$, and $P(-,-)$.

Evaluating the above expressions using states belonging to the first class, where $\psi(x,x')=\psi(-x,-x')$, we have

$$P(+,+) = \frac{1}{2}(1+\Delta), \quad P(-,-) = \frac{1}{2}(1-\Delta), \tag{21}$$

and $P(+,-)=P(-,+)=0$; here

$$\Delta = \mathrm{Re}\left\{\int\int dx_1 dx_2 \psi(x_1,x_2)\psi^*(-x_1,x_2)\right\} = \sum_n \lambda_{2n}^2 - \sum_n \lambda_{2n+1}^2. \tag{22}$$

The quantity Δ is the difference between the weight of the even-even contribution ($\Sigma_n \lambda_{2n}^2$) and that of the odd-odd contribution ($\Sigma_n \lambda_{2n+1}^2$) in the Schmidt decomposition of the two-photon state. When $\Delta=1$, photon pairs are always detected by the detectors D_1^+ and D_2^+ (even-even); when $\Delta=-1$, photon pairs are always detected by the detectors D_1^- and D_2^- (odd-odd). In both of these cases the state is separable in parity space. When $|\Delta|\neq 1$ photon pairs are detected by the detectors D_1^+ and D_2^+ (even-even) or by D_1^- and D_2^- (odd-odd); the photon pairs are never detected by the detectors D_1^+ and D_2^- (even-odd) or by D_1^- and D_2^+ (odd-even). In particular, $\Delta\to 0$ for the EPR state, and the ratio of even-even to odd-odd detections is 1.

As a concrete example of state functions with $\psi(x,x')=\psi(-x,-x')$, consider the two-photon state characterized by a state function of the form (see Appendix A)

$$\psi(x,x') = A\exp\left[-\left(\frac{x+x'}{l_1}\right)^2\right]\exp\left[-\left(\frac{x-x'}{l_2}\right)^2\right], \tag{23}$$

with the normalization constant $|A|^2=4/\pi l_1 l_2$, which allows us to obtain an analytic formula for Δ:

$$\Delta = \frac{2l_2/l_1}{1+(l_2/l_1)^2}. \tag{24}$$

Two limits are of particular interest: (1) the highly entangled state $l_2 \ll l_1 \to \Delta \approx 0$, where we have $P(+,+)=P(-,-)=\frac{1}{2}$ and all the singles rates are equal to $\frac{1}{2}$ and (2) the separable state $l_1=l_2\to\Delta=1$, where we have $P(+,+)=1$, $P(-,-)=0$, and the singles rates are $P(D_1^+)=P(D_2^+)=1$ and $P(D_1^-)=P(D_2^-)=0$. The results of these two limits correspond to Stern-Gerlach measurements with the angle settings $\theta_1=\theta_2=0$ applied to the maximally entangled state $\frac{1}{\sqrt{2}}\{|\uparrow\uparrow\rangle+|\downarrow\downarrow\rangle\}$ and the factorizable state $|\uparrow\uparrow\rangle$, respectively.

Similar results to those above are obtained when the second class of two-photon states $[\psi(x,x')=-\psi(-x,-x')]$ is considered, with obvious modifications. Thus, for a maximally entangled state in parity space in this class we have $P(+,-)=P(-,+)=\frac{1}{2}$ and $P(+,+)=P(-,-)=0$, while in the separable case we have $P(+,-)=1$ and $P(-,+)=P(+,+)=P(-,-)=0$ [or, alternatively, $P(-,+)=1$ and $P(+,-)=P(+,+)=P(-,-)=0$]. The results of these two limits correspond to Stern-Gerlach measurements with the angle settings $\theta_1=\theta_2=0$ applied to the maximally entangled state $\frac{1}{\sqrt{2}}\{|\uparrow\downarrow\rangle+|\downarrow\uparrow\rangle\}$ and the factorizable state $|\uparrow\downarrow\rangle$, respectively. In Appendix A we discuss in more detail how to produce all four Bell states. Thus, one may, in principle, produce states corresponding to arbitrary two-qubit states in parity space through superpositions of them.

V. VIOLATION OF BELL'S INEQUALITY IN TWO-PHOTON PARITY SPACE

We are now in a position to describe our scheme for testing the CHSH inequality using the spatial parameters of the photon pairs. Implementing a test of this inequality violation requires an SO(2) operator for each photon [Fig. 3(c) or 4(b)]. Two proposed setups are shown in Fig. 6. In the first proposed setup each photon is sent through an implementation of an SO(2) operator [Fig. 3(c)] followed by a parity analyzer. In the second proposed setup each photon passes through a parity analyzer followed by an SO(2) operator [Fig. 4(b)]. The parameters of the SO(2) operators are θ_1 and θ_2 for photons 1 and 2, respectively. It is assumed that θ_1 and θ_2 are set locally and their locations are spacelike separated to outlaw any possible communication between the two sites. The detectors at the two exit ports for each photon are denoted as in the previous section (Fig. 5). The two implementations yield identical outcomes and the following analysis applies to both.

Coincidence measurements between pairs of detectors allow us to compute a parity correlation function $E_p(\theta_1,\theta_2)$ given by

$$E_p(\theta_1,\theta_2) = P(+,+) - P(+,-) - P(-,+) + P(-,-), \tag{25}$$

where $-1\leq E_p(\theta_1,\theta_2)\leq 1$, with the limits corresponding to correlated and anticorrelated parity measurements. Using the two-photon state specified in Eq. (1), and assuming that $\psi(x,x')=\psi(-x,-x')$, one may derive an analytical expression for E_p

$$E_p(\theta_1,\theta_2) = \cos(\theta_1+\theta_2) + (1-\mathsf{P})\sin\theta_1\sin\theta_2, \tag{26}$$

where the parameter P is given by

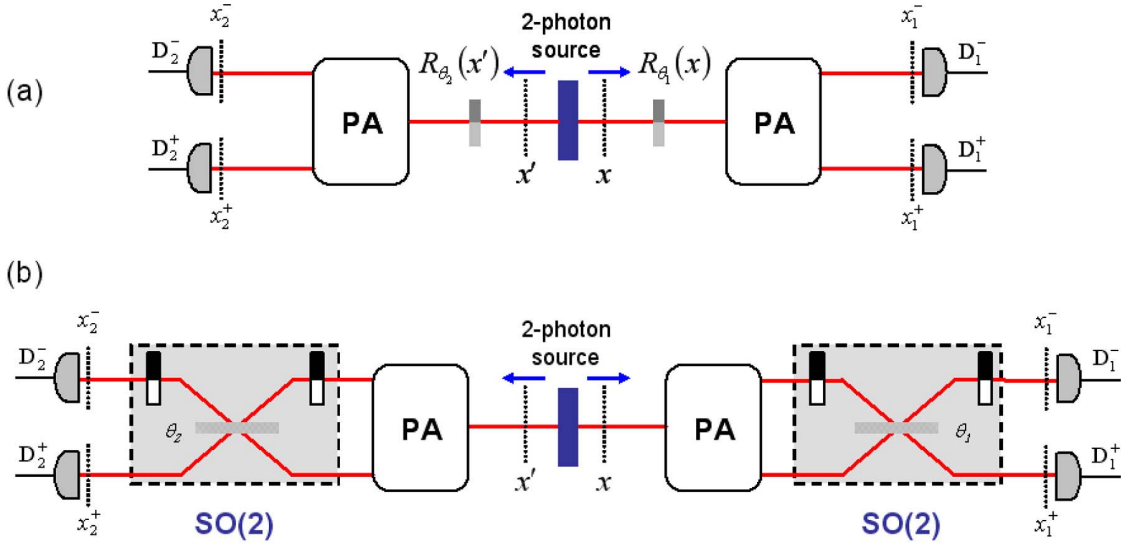

FIG. 6. (Color online) Arrangements for demonstrating a violation of Bell's inequality for continuous spatial variables. (a) The two-photon source directs each photon into an SO(2) operator, $R_{\theta_1}(x)$ and $R_{\theta_2}(x')$ [Figs. 3(b) and 3(c)] followed by two parity analyzers and detectors, as in Fig. 5. The two photons undergo rotations of θ_1 and θ_2 in parity space. (b) The two-photon source directs each photon into a parity analyzer (PA) followed by the SO(2) operator shown in Fig. 4(b).

$$\mathsf{P} = \int\int dx_1 dx_2 |\psi(x_1,x_2)|^2 h(x_1)h(x_2), \tag{27}$$

which is equal to the total area of $|\psi(x_1,x_2)|^2$ after twice the area of its second and fourth quadrants in the x_1-x_2 space are subtracted from it. The first term in Eq. (26) is the result expected for an ideal maximally entangled EPRB state [Eq. (2)], while the second term quantifies the deviation from the ideal condition.

An entangled state [$\psi(x_1,x_2)\to\delta(x_1-x_2)$, or $l_2\to 0$ in Eq. (23)] yields $\mathsf{P}=1$ and $E_p(\theta_1,\theta_2)=\cos(\theta_1+\theta_2)$, resulting in a maximal violation of the CHSH inequality. A factorizable state [$\psi(x_1,x_2)\to\psi_1(x_1)\psi_2(x_2)$, or $l_1=l_2$ in Eq. (23)] yields $\mathsf{P}=0$, and E_p factorizes as expected, $E_p(\theta_1,\theta_2)=\cos\theta_1\cos\theta_2$. In this case the maximal attainable value of the Bell operator is 2, and the CHSH inequality is not violated.

The maximal value $\mathcal{B}_{\max}=2\sqrt{2}$ of the Bell operator for an entangled state may be achieved at the settings $\theta_1=\theta_2=\frac{\pi}{8}$ and $\theta_1'=\theta_2'=\frac{13\pi}{8}$, for example. If we fix these settings while varying the parameter P, the Bell operator for the two-photon state is $\mathcal{B}=\frac{1}{2}(1+\mathsf{P})\mathcal{B}_{\max}$, which is plotted in Fig. 7(a) (dashed curve). Obviously the inequality ceases to be violated ($\mathcal{B}<2$) when $\mathsf{P}<\sqrt{2}-1$. However, one may choose to change the four settings $(\theta_1,\theta_1',\theta_2,\theta_2')$ in order to maximize the violation of the inequality for each value of P, and the resulting values of the Bell operator are plotted in Fig. 7(a) (solid curve). If this procedure is followed, the EPR state always yields a violation of the CHSH inequality in parity space. The solid curve in Fig. 7(a) may in fact be fitted to the relation

$$\mathcal{B}=2\sqrt{1+\mathsf{P}^2}. \tag{28}$$

In Fig. 7(b) we plot the value of the parameter P for the Gaussian state in Eq. (23) as a function of the ratio l_2/l_1.

Thus far, the parameter P appears to be a good candidate to quantify the entanglement of the EPR state in parity space since it varies monotonically from 1 for the maximally entangled state to 0 for the factorizable state, and it quantifies the amount of violation of the CHSH inequality in parity space. This intuition can be placed on more solid ground by

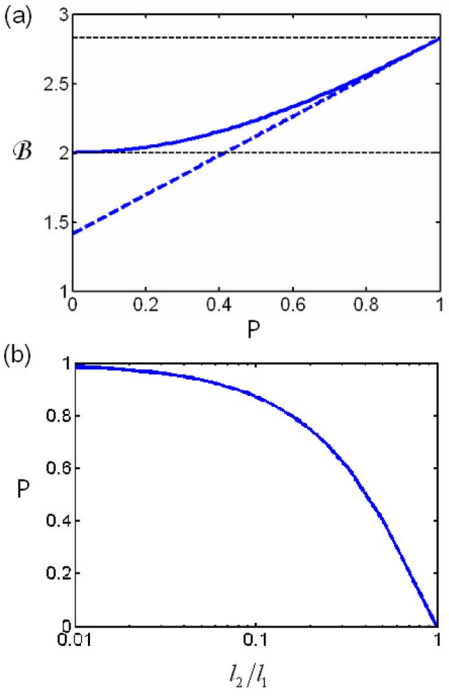

FIG. 7. (Color online) (a) The Bell operator $\mathcal{B}$ for the CHSH inequality as a function of the parity concurrence P. The dashed line is calculated for fixed parameter settings $(\theta_1=\theta_2=\frac{\pi}{8}$ and $\theta_1'=\theta_2'=\frac{13\pi}{8})$, whereas the solid curve is calculated by optimizing the parameter settings for maximal value of the Bell operator. (b) The value of P for the Gaussian state in Eq. (23) as a function of l_2/l_1.

comparing the conceptual development so far with the EPRB case. An arbitrary two-spin-$\frac{1}{2}$ state (nonmaximally entangled EPRB state) may always be reduced to the Schmidt form

$$|\Psi\rangle = \lambda_0|\uparrow\uparrow\rangle + \lambda_1|\downarrow\downarrow\rangle, \tag{29}$$

with the spin correlation function

$$E_s(\theta_1,\theta_2) = \cos(\theta_1+\theta_2) + (1-C)\sin\theta_1 \sin\theta_2, \tag{30}$$

where

$$C = 2\lambda_0\lambda_1 \tag{31}$$

is the concurrence, as defined by Wootters [72–74]. The correspondence between Eq. (30) and Eq. (26) is obvious. The Bell operator for the CHSH inequality in spin space is

$$\mathcal{B} = 2\sqrt{1+C^2}. \tag{32}$$

Further insight into the relation between the degree of parity entanglement P and concurrence C may be gained after deriving an alternative expression for P by substituting the Schmidt form [Eq. (18)] into the definition of P [Eq. (27)], yielding

$$\mathsf{P} = \sum_{n,m=0,1,2,\ldots} \lambda_n\lambda_m \mathrm{Re}\{h^{(\phi)}_{n,m}h^{(\xi)}_{n,m}\}, \tag{33}$$

where the coefficients $h^{(\phi)}_{n,m}$ and $h^{(\xi)}_{n,m}$ are the components of the operator $h(x)$ in the $\{\phi_n(x)\}$ and $\{\xi_n(x)\}$ bases, respectively,

$$h^{(\phi)}_{n,m} = \int dx \phi_n(x)h(x)\phi^*_m(x),$$

$$h^{(\xi)}_{n,m} = \int dx \xi_n(x)h(x)\xi^*_m(x). \tag{34}$$

Let us consider a few examples of forms of the Schmidt decomposition. For a 2×2 system (i.e., both bases comprise two functions only), we have the degree of parity entanglement

$$\mathsf{P} = 2\lambda_0\lambda_1 \mathrm{Re}\{h^{(\phi)}_{0,1}h^{(\xi)}_{0,1}\}. \tag{35}$$

The quantity $\mathrm{Re}\{h^{(\phi)}_{0,1}h^{(\xi)}_{0,1}\}$ achieves a maximum value of 1 when $\phi_0(x)=h(x)\phi_1(x)$ and $\xi_0(x)=h(x)\xi_1(x)$ (i.e., the space spanned by these bases are closed under the parity-flip operation), resulting in the expression

$$\mathsf{P} = 2\lambda_0\lambda_1, \tag{36}$$

which reaches a maximum value of 1 when $\lambda_0=\lambda_1=\frac{1}{\sqrt{2}}$ for a maximally entangled state.

Consider now the case of a 2×3 system (i.e., both bases comprise three functions), where the degree of parity entanglement is

$$\mathsf{P} = 2(\lambda_0\lambda_1 \mathrm{Re}\{h^{(\phi)}_{0,1}h^{(\xi)}_{0,1}\} + \lambda_1\lambda_2 \mathrm{Re}\{h^{(\phi)}_{1,2}h^{(\xi)}_{1,2}\}). \tag{37}$$

In this case, when $\lambda_0=\lambda_1=\lambda_2=\frac{1}{\sqrt{3}}$, $\mathsf{P}^{\mathrm{m.e.}}$ reaches a maximum value of $\frac{2}{3}$ (and not 1) when $\phi_1(x)=[\alpha^*\phi_0(x)+\beta^*\phi_2(x)]\,h(x)$ and $\xi_1(x)=[\alpha\xi_0(x)+\beta\xi_2(x)]\,h(x)$, where $|\alpha|^2+|\beta|^2=1$. Note that since the dimension of the space describing each photon is odd, they cannot be closed under the parity-flip operation, which results in a nominally maximally entangled state, not maximal violation of the CHSH inequality in parity space, although it could ostensibly produce a maximal violation in an alternatively constructed space. In fact, one can show that, in general, the maximal value of the degree of parity entanglement for maximally entangled states ($\lambda_n=\frac{1}{\sqrt{N}}$, $n=0\ldots N-1$, where N is the number of terms in the Schmidt decomposition), is given by

$$\mathsf{P}_{\max} = \begin{cases} 1, & \forall N \text{ even}, \\ 1-\dfrac{1}{N}, & \forall N \text{ odd}. \end{cases} \tag{38}$$

Spin Space	Parity Space
$\lvert\uparrow\rangle$	$\lvert e\rangle$
$\lvert\downarrow\rangle$	$\lvert o\rangle$
σ_x	S_x Parity Flipper
σ_z	S_z Spatial Flipper
$i\sigma_y$	iS_y SF + PF
EPRB state $\frac{1}{\sqrt{2}}\{\lvert\uparrow\uparrow\rangle+\lvert\downarrow\downarrow\rangle\}$	EPR state $\iint dxdx'\,\delta(x-x')\lvert 1_x,1_{x'}\rangle$
Stern-Gerlach Device	Parity Analyzer
Concurrence C	Degree of Parity Entanglement P

FIG. 8. A table showing the identification of the states, operators, and variables in the traditional spin space with those of the parity space discussed in this paper.

VI. DISCUSSION AND CONCLUSION

It is most convenient to pose the paradoxes of quantum mechanics and the problems of quantum information processing in the language of discretized systems, in particular using a spin-$\frac{1}{2}$ formalism. Previous work on higher-dimensional Hilbert spaces (so far up to 3) has relied on the signal and idler photons' orbital angular momenta. While this

approach is implemented in the spatial domain, it is distinct from the scheme that we have proposed here. (1) The work pursued so far using orbital angular momentum truncates the angular momentum space of entangled photons to a two- or three-dimensional space for each photon, while our approach, which makes use of spatial-parity space, does not truncate the space. (2) The experimental implementation of operators on spatial parity are considerably simpler than those on orbital angular momentum space. For example, the conversion of the parity of a photon, or more generally rotation in parity space, is achieved with a simple phase plate, whereas the same process requires more involved arrangements in angular-momentum space. (3) Finally, the angular momentum approach requires 2D optical fields in contrast to our arrangement, which makes use of 1D only. It is also important to note the difference between this work and that of Rarity and Tapster [9], which relied on discretizing the spatial field by using pinholes, while our approach makes use of the full wave front of the photon pairs. We have summarized the isomorphism between the familiar operators and states in spin-$\frac{1}{2}$ space, heavily used in quantum information processing, and the corresponding spatial-parity operators and states in the table depicted in Fig. 8.

While we have made several (realistic) assumptions (see Appendix A) that allow us to consider the 1D spatial domain, one could also put the second spatial dimension to work. One may also consider the possibility of studying entanglement in the temporal or polarization domain, alongside the 2D spatial-parity space, which would add a further dimension to the hyperentangled states studied by Barreiro *et al.* [75].

Using the spatial-parity approach, one can consider quantum cryptography or quantum teleportation in the spatial-parity domain. While we have suggested some concrete optical arrangements, their design was chosen for pedagogical reasons, and many other alternative designs may be considered that achieve the same goals while accommodating the requirements of the specific application.

In conclusion, we have proposed an experimental scheme that allows for the violation of Bell's inequality, and hence demonstrating quantum nonlocality, that utilizes continuous spatial quantum variables. The experimental arrangement is particularly simple and straightforward, in contrast to previous proposals. The source is the process of optical spontaneous parametric downconversion, and the continuous spatial parameters of the signal and idler photons are manipulated using simple optical components to implement a Bell operator. Each photon traverses a unitary optical system that is described with a single parameter representing a rotation in a parity space constructed over the spatial parameter.

ACKNOWLEDGMENTS

A.F.A. acknowledges the generous support and encouragement of Y. Fink and J. D. Joannopoulos. This work was supported by a U. S. Army Research Office (ARO) Multidisciplinary University Research Initiative (MURI) Grant; the Center for Subsurface Sensing and Imaging Systems (CenSSIS), an NSF Engineering Research Center; and the National Aeronautics and Space Administration (NASA) under United States Air Force Contract No. FA8721-05-C-0002 to M.I.T. Lincoln Laboratory. Opinions, interpretations, recommendations, and conclusions are those of the authors and are not necessarily endorsed by the United States Government.

APPENDIX A: 1D STATE PRODUCED BY SPDC IN THE SPATIAL DOMAIN

The quantum state representing the two-photon field produced by SPDC from a nonlinear crystal of thickness L is given by [46,76–79]

$$|\Psi\rangle = \int\int d\mathbf{q}_s d\mathbf{q}_i \tilde{E}_p(q_s^x + q_i^x, q_s^y + q_i^y)\tilde{\chi}(\mathbf{q}_s, \mathbf{q}_i)|1_{\mathbf{q}_s}, 1_{\mathbf{q}_i}\rangle, \tag{A1}$$

where $\mathbf{q}_t = (q_t^x, q_t^y)$, and $k_t = 2\pi/\lambda_t$, $t = p, s, i$, are the transverse momentum vectors and total momenta of the pump, signal, and idler photons, respectively (λ is the wavelength inside the crystal); $\tilde{E}_p(q_p^x, q_p^y)$ is the 2D Fourier transform of the pump spatial profile $E_p(x,y)$ at the entrance to the nonlinear crystal; the phase-matching function $\tilde{\chi}$ depends on the axial wave-number mismatch $\Delta k_z = k_p^z - k_s^z - k_i^z$: $\tilde{\chi}(\mathbf{q}_s, \mathbf{q}_i) \propto \exp(iL\Delta k_z/2)\mathrm{sinc}(L\Delta k_z/2\pi)$; here

$$k_p^z = \sqrt{k_p^2 - (q_s^x + q_i^x)^2 - (q_s^y + q_i^y)^2},$$

$$k_s^z = \sqrt{k_s^2 - (q_s^x)^2 - (q_s^y)^2}, \quad k_i^z = \sqrt{k_i^2 - (q_i^x)^2 - (q_i^y)^2}.$$

Assuming type-I collinear phase-matched SPDC and the paraxial approximation, we have $\Delta k_z \approx [(q_s^x - q_i^x)^2 + (q_s^y - q_i^y)^2]/2k_p$. The phase-matching function $\tilde{\chi}(\mathbf{q}_s, \mathbf{q}_i)$ may then be separated, with very good approximation, to

$$\begin{aligned}\tilde{\chi}(\mathbf{q}_s, \mathbf{q}_i) &= \tilde{\chi}_2(q_s^x - q_i^x, q_s^y - q_i^y) \\ &\approx \tilde{\chi}_1(q_s^x - q_i^x)\tilde{\chi}_1(q_s^y - q_i^y),\end{aligned} \tag{A2}$$

where $\tilde{\chi}_1(q) = \exp(i\pi Lq^2/2\lambda_p)\mathrm{sinc}(Lq^2/2\lambda_p)$. The quality of this approximation is determined by calculating the overlap integral

$$\eta = \frac{\left|\int\int dq^x dq^y \tilde{\chi}_2(q^x, q^y)\tilde{\chi}_1^*(q^x)\tilde{\chi}_1^*(q^y)\right|}{\sqrt{\int\int dq^x dq^y |\tilde{\chi}_2(q^x, q^y)|^2}\sqrt{\int\int dq^x dq^y |\tilde{\chi}_1(q^x)\tilde{\chi}_1(q^y)|^2}}. \tag{A3}$$

For the range of values of L/λ_p of interest, the overlap integral η always exceeds 94%.

In this paper we only consider pump spatial profiles that are separable, $\tilde{E}_p(q_p^x, q_p^y) = \tilde{E}_x(q_p^x)\tilde{E}_y(q_p^y)$, or equivalently $E_p(x,y) = E_x(x)E_y(y)$ (the effect of using pump profiles that are nonseparable in x and y will be considered elsewhere), whereupon the quantum state becomes

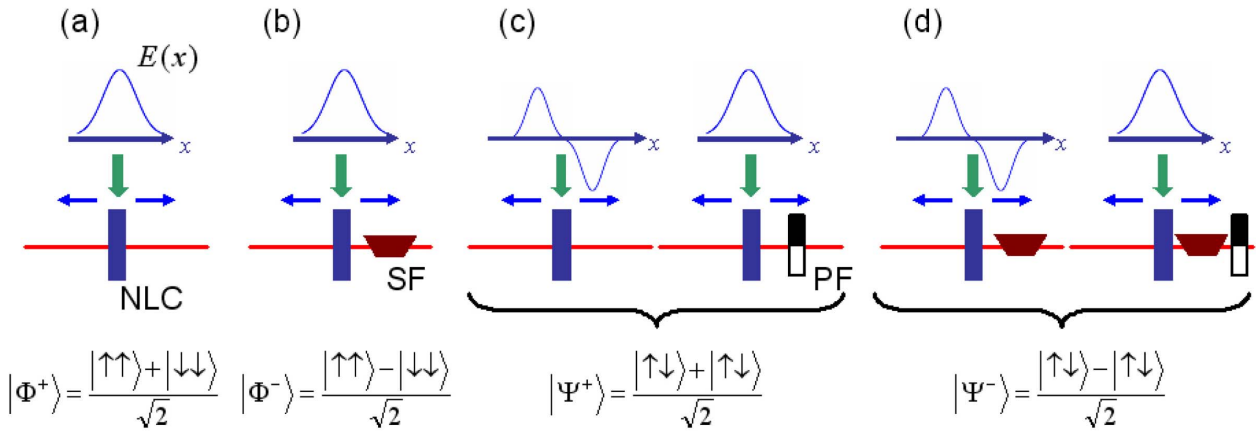

FIG. 9. (Color online) Producing the four Bell states in parity space. (a) The Bell state $|\Phi^+\rangle$ is produced using type-I collinear degenerate SPDC from a nonlinear crystal (NLC) when the pump has an even spatial profile. (b) The Bell state $|\Phi^-\rangle$ is produced when a spatial flipper (SF) is placed in the path of one of the photons produced in (a). (c) The Bell state $|\Psi^+\rangle$ is produced using the setup in (a) by either using a pump with an odd spatial profile or placing a parity flipper (PF) in the path of one photon while using an even pump. (d) The Bell state $|\Psi^-\rangle$ is produced using the two setups in (c) in conjunction with a spatial flipper (SF) placed in the path of one of the photons.

$$|\Psi\rangle = \int\int dq_s^x dq_i^x \tilde{E}_x(q_s^x + q_i^x)\chi_1(q_s^x - q_i^x)|1_{q_s^x}, 1_{q_i^x}\rangle \otimes \int\int dq_s^y dq_i^y \tilde{E}_x(q_s^y + q_i^y)\chi_1(q_s^y - q_i^y)|1_{q_s^y}, 1_{q_i^y}\rangle = |\Psi^x\rangle \otimes |\Psi^y\rangle. \quad \text{(A4)}$$

Assuming that none of the optical components in the experimental arrangements leads to mixing of the x and y coordinates, we may trace out the $|\Psi^y\rangle$ subspace, leaving only $|\Psi^x\rangle$. From here on, we drop the "x" superscript and it is understood that we have only one spatial dimension.

In the spatial domain, the 1D two-photon state is now the EPR state given by Eq. (1) with $\psi(x,x') = \int dx'' E(x'')\chi_1(x - x'', x - x'')$; $\chi_1(x,x')$ is the linear shift-invariant joint probability amplitude of emitting the signal and idler photons from x and x', respectively, from a point in the pump beam (and is the 2D inverse Fourier transform of $\tilde{\chi}_1$). Since the phase-matching function $\tilde{\chi}_1$ takes the form $\tilde{\chi}_1(q_s - q_i)$, its 2D Fourier transform is $\chi(x,x') = \delta(x + x')\chi_1\left(\frac{x-x'}{2}\right)$, and the state function becomes

$$\psi(x,x') = E\left(\frac{x+x'}{2}\right)\chi_1\left(\frac{x-x'}{2}\right). \quad \text{(A5)}$$

In other words, the state function is separable along the $x + x'$ and $x - x'$ axes. The width of the function χ_1 is of the order $\sqrt{L\lambda_p}/8$ which is usually $\ll W$ (the width of the pump function E). Note that $\chi_1(x,x')$ is invariant under inversion through the origin of the x-x' plane: $\chi_1(x,x') = \chi_1(-x,-x')$. As a result the behavior of the state function $\psi(x,x')$ in Eq. (A5) under inversion through this origin depends on $E(x)$. If the pump spatial profile is even, $E(x) = E(-x)$, then $\psi(x,x') = \psi(-x,-x')$; if $E(x) = -E(-x)$, then $\psi(x,x') = -\psi(-x,-x')$.

The state used in this paper for computational purposes [given in Eq. (23)] was arrived at by assuming a pump with a Gaussian profile of width $l_1 = W$, and approximating the phase-matching function χ_1 with a Gaussian function of width $l_2 = \sqrt{\lambda_p L}/8$. The ideal EPR state is arrived at when (1) the nonlinear-crystal thickness decreases $L \to 0$, so that $\chi_1\left(\frac{x-x'}{2}\right) \to \delta(x - x')$ and (2) the pump width increases $W \to \infty$, so that $E\left(\frac{x+x'}{2}\right) \to 1$, in which case $\psi(x,x') \to \delta(x - x')$.

Using this approach, we can generate all four Bell states $\{|\Phi^+\rangle, |\Phi^-\rangle, |\Psi^+\rangle, |\Psi^-\rangle\}$. In Sec. IV we discussed how the Bell state $|\Phi^+\rangle = \frac{1}{\sqrt{2}}\{|ee\rangle + |oo\rangle\}$ is produced when a pump having an even spatial profile is used [Fig. 9(a)]. Placing a spatial flipper (SF) [Fig. 1(b)], corresponding to S_z, in the path of one of the photons results in the Bell state $|\Phi^-\rangle = (\mathbb{I} \otimes S_z)|\Phi^+\rangle = \frac{1}{\sqrt{2}}\{|ee\rangle - |oo\rangle\}$ [Fig. 9(b)]. To generate the Bell state $|\Psi^+\rangle = \frac{1}{\sqrt{2}}\{|eo\rangle + |oe\rangle\}$ one may either: (1) replace the even pump used to generate $|\Phi^+\rangle$ with an odd pump or (2) retain an even pump while placing a parity flipper (PF) [Fig. 1(a)], corresponding to S_x, in the path of one of the photons [Fig. 9(c)], $|\Psi^+\rangle = (\mathbb{I} \otimes S_x)|\Phi^+\rangle$. The final Bell state $|\Psi^-\rangle$ is obtained using either approach to produce $|\Psi^+\rangle$, after a spatial flipper is placed in the path of one of the photons [Fig. 9(d)], $|\Psi^-\rangle = (\mathbb{I} \otimes S_z)|\Psi^+\rangle$.

APPENDIX B: SPATIAL PARITY OPERATORS

In the spatial domain we define the parity operators S_k, $k = x, y, z$, which correspond to the pseudospin operators s_k in the Fock basis in Eq. (4) and have the commutation relations $[S_i, S_j] = i2\epsilon_{ijk}S_k$, where ϵ_{ijk} is the antisymmetric tensor. In the first level of description, namely, in the spatial domain [corresponding to the state given in Eq. (5)], each operator is associated with a linear, unitary optical system characterized by an impulse response function. The operators have the general form

$$S_k = \int\int dx dx' h_k(x,x')|1_x\rangle\langle 1_{x'}|, \quad k = x,y,z, \quad \text{(B1)}$$

where $h_k(x,x')$ is the impulse response function of the associated optical system given explicitly by

$$h_x(x,x') = \sum_n [\phi_{2n+1}(x)\phi_{2n}^*(x') + \phi_{2n}(x)\phi_{2n+1}^*(x')],$$

$$h_y(x,x') = i\sum_n [\phi_{2n+1}(x)\phi_{2n}^*(x') - \phi_{2n}(x)\phi_{2n+1}^*(x')],$$

$$h_z(x,x') = \sum_n [\phi_{2n}(x)\phi_{2n}^*(x') - \phi_{2n+1}(x)\phi_{2n+1}^*(x')]. \tag{B2}$$

The unity operator $\mathbb{I}$ is associated with an optical system having the impulse response function $h_{\mathbb{I}}(x,x') = \Sigma_n \phi_n(x)\phi_n^*(x') = \delta(x-x')$.

When a parity operator is applied to the state in Eq. (5), the result is

$$S_k|\Psi\rangle = \int dx \psi'(x)|1_x\rangle, \tag{B3}$$

where $\psi'(x) = \int dx' h_k(x,x')\psi(x')$. The parity operators' commutation relations imply that the associated impulse response functions are characterized by the relation

$$\int dx'' h_i(x,x'')h_j(x'',x') = i\epsilon_{ijk}h_k(x,x'). \tag{B4}$$

Furthermore, since the parity operators are Hermitian and unitary, we have $h_i(x,x') = h_i^*(x',x)$ and $\int dx'' h_i(x,x'')h_i(x'',x') = \delta(x-x')$, $i=x,y,z$, respectively. We may also define parity "raising" S^+ and "lowering" S^- operators associated with optical systems having impulse response functions $h^+(x,x') = \Sigma_n \phi_{2n+1}(x)\phi_{2n}^*(x')$ and $h^-(x,x') = \Sigma_n \phi_{2n}(x)\phi_{2n+1}^*(x')$, respectively. The raising operator changes an even-parity mode to an odd-parity mode, and vice versa for the lowering operator.

The second level of description, in the discretized space of spatial eigenmodes [corresponding to Eq. (7)], uses the identification $\int dx \phi_n(x)|1_x\rangle = |n\rangle$ to recast the parity operators into the identical form of the pseudo-spin operators of Eq. (4). When a parity operator is applied to the state in Eq. (7), the result is

$$S_k|\Psi\rangle = \sum_n c_n'|n\rangle, \tag{B5}$$

where $c_n' = \Sigma_m \alpha_{n,m}^k c_m$ and

$$\alpha_{n,m}^k = \int\int dx dx' \phi_n^*(x)h_k(x,x')\phi_m(x'). \tag{B6}$$

In the third level of description, that of the 2D spatial parity space [corresponding to Eq. (8)], the parity operators can be recast into 2×2 matrices isomorphic to the Pauli spin-$\frac{1}{2}$ operators. When a parity operator is applied to the state in Eq. (8), the result is

$$S_k|\Psi\rangle = (\eta_{ee}^k\alpha + \eta_{eo}^k\beta)|e'\rangle + (\eta_{oe}^k\alpha + \eta_{oo}^k\beta)|o'\rangle, \tag{B7}$$

where η_{ee}^k, η_{eo}^k, η_{oe}^k, and η_{oo}^k are the components of the 2×2 representation of S_k, and $\{|e'\rangle, |o'\rangle\}$ is the new transformed basis. The parity operator S_x, for example, when applied to the state in Eq. (8), yields

$$S_x|\Psi\rangle = \sum_{n=0}^{\infty} c_{2n+1}|2n\rangle + \sum_{n=0}^{\infty} c_{2n}|2n+1\rangle = \beta|e'\rangle + \alpha|o'\rangle. \tag{B8}$$

APPENDIX C: LINEAR SPACES CLOSED UNDER PARITY FLIP

Consider the Hermite-Gaussian basis $\{\phi_n(x)\}$ consisting of an alternating series of even and odd functions. Since the set is complete over L_2, and the even and odd functions are orthogonal, we have

$$R_\pi(x)\phi_{2n}(x) = \sum_{m=0}^{\infty} R_{2n,2m+1}\phi_{2m+1}(x),$$

$$R_\pi(x)\phi_{2n+1}(x) = \sum_{m=0}^{\infty} R_{2n+1,2m}\phi_{2m}(x), \tag{C1}$$

where $R_{n,m} = \int dx \phi_n^*(x)R_\pi(x)\phi_m(x)$ and $R_{n,m} = R_{m,n}^*$. In other words, the parity flip of an *even* function can be written as a superposition of *odd* functions, and vice versa. Furthermore, since $R_\pi(x)R_\pi(x)\phi_n(x) = \phi_n(x)$, $\forall n$, we have

$$\sum_{m=0}^{\infty} |R_{n,m}|^2 = 1, \quad \forall n. \tag{C2}$$

We denote every subspace of L_2 where the parity flip of every even function can be written as a superposition of the odd basis functions (and vice versa) *closed under parity flip*. This property holds for any complete basis over L_2 since the basis can be transformed through a unitary transformation to the Hermite-Gaussian basis for which this property holds. This property may also apply to suitably defined subspaces of L_2.

Consider a linear vector space of dimension $2N$ (a subspace of L_2, where N may be infinite) with a basis $\{\sigma_n(x)\}_{n=0}^{2N-1}$ consisting of alternating even and odd orthonormal functions (not necessarily the Hermite-Gaussian functions). Any even (odd) function in this space can be written as a superposition of the even (odd) basis functions $\{\sigma_{2n}(x)\}$ ($\{\sigma_{2n+1}(x)\}$). The space is closed under the parity flip operation $R_\pi(x)$ if

$$R_\pi(x)\begin{pmatrix}\sigma_0(x)\\ \sigma_2(x)\\ \vdots\end{pmatrix} = \mathbf{U}_N\begin{pmatrix}\sigma_1(x)\\ \sigma_3(x)\\ \vdots\end{pmatrix}, \tag{C3}$$

where $\mathbf{U}_N$ is an SU(N) transformation. The right-hand side of Eq. (C3) is a column of transformed odd basis functions that we denote $\{\sigma_{2n+1}'(x)\}$. We may now define a new orthonormal basis for this subspace of L_2 consisting of the even-odd alternating functions $\{\sigma_0(x), \sigma_1'(x), \sigma_2(x), \sigma_3'(x), \ldots\}$. Using this new basis, the operator $R_\pi(x)$ has the following effect:

$\sigma'_{2n+1}(x)=R_\pi(x)\sigma_{2n}(x)$ and $\sigma'_{2n}(x)=R_\pi(x)\sigma'_{2n+1}(x)$, $\forall n$, i.e., $R_\pi(x)\delta(x-x')$ is the impulse response function of an optical system associated with the parity operator S_x. We thus conclude that if a space is closed under parity flip in the above defined sense, there is always a basis in which $R_\pi(x)$ corresponds to the parity operator S_x. Finally, we note that a subspace of L_2 with odd dimensionality cannot be closed under the parity-flip operation.

[1] A. Einstein, B. Podolsky, and N. Rosen, Phys. Rev. **47**, 777 (1935).
[2] N. Bohr, Phys. Rev. **48**, 696 (1935).
[3] D. Bohm, *Quantum Theory* (Prentice-Hall, New York, 1951).
[4] J. S. Bell, Physics (Long Island City, N.Y.) **1**, 195 (1964).
[5] J. F. Clauser, M. A. Horne, A. Shimony, and R. A. Holt, Phys. Rev. Lett. **23**, 880 (1969).
[6] A. Aspect, P. Grangier, and G. Roger, Phys. Rev. Lett. **47**, 460 (1981).
[7] A. Aspect, P. Grangier, and G. Roger, Phys. Rev. Lett. **49**, 91 (1982).
[8] A. Aspect, J. Dalibard, and G. Roger, Phys. Rev. Lett. **49**, 1804 (1982).
[9] J. G. Rarity and P. R. Tapster, Phys. Rev. Lett. **64**, 2495 (1990).
[10] P. R. Tapster, J. G. Rarity, and P. C. M. Owens, Phys. Rev. Lett. **73**, 1923 (1994).
[11] W. Tittel, J. Brendel, H. Zbinden, and N. Gisin, Phys. Rev. Lett. **81**, 3563 (1998).
[12] G. Weihs, T. Jennewein, C. Simon, H. Weinfurter, and A. Zeilinger, Phys. Rev. Lett. **81**, 5039 (1998).
[13] T. Jennewein, C. Simon, G. Weihs, H. Weinfurter, and A. Zeilinger, Phys. Rev. Lett. **84**, 4729 (2000).
[14] D. S. Naik, C. G. Peterson, A. G. White, A. J. Berglund, and P. G. Kwiat, Phys. Rev. Lett. **84**, 4733 (2000).
[15] W. Tittel, J. Brendel, H. Zbinden, and N. Gisin, Phys. Rev. Lett. **84**, 4737 (2000).
[16] C. H. Bennett, G. Brassard, C. Crépeau, R. Jozsa, A. Peres, and W. K. Wootters, Phys. Rev. Lett. **70**, 1895 (1993).
[17] D. Bouwmeester, J.-W. Pan, K. Mattle, M. Eibl, H. Weinfurter, and A. Zeilinger, Nature (London) **390**, 575 (1997).
[18] D. Boschi, S. Branca, F. DeMartini, L. Hardy, and S. Popescu, Phys. Rev. Lett. **80**, 1121 (1998).
[19] *The Physics of Quantum Information*, edited by D. Bouwmeester, A. K. Ekert, and A. Zeilinger (Springer, New York, 2000).
[20] T. E. Kiess, Y. H. Shih, A. V. Sergienko, and C. O. Alley, Phys. Rev. Lett. **71**, 3893 (1993).
[21] P. G. Kwiat, K. Mattle, H. Weinfurter, A. Zeilinger, A. V. Sergienko, and Y. Shih, Phys. Rev. Lett. **75**, 4337 (1995).
[22] P. G. Kwiat, E. Waks, A. G. White, I. Appelbaum, and P. H. Eberhard, Phys. Rev. A **60**, R773 (1999).
[23] J. D. Franson, Phys. Rev. Lett. **62**, 2205 (1989).
[24] Y. H. Shih, A. V. Sergienko, and M. H. Rubin, Phys. Rev. A **47**, 1288 (1993).
[25] P. G. Kwiat, A. M. Steinberg, and R. Y. Chiao, Phys. Rev. A **47**, R2472 (1993).
[26] S. L. Braunstein and P. van Loock, Rev. Mod. Phys. **77**, 513 (2005).
[27] M. D. Reid and P. D. Drummond, Phys. Rev. Lett. **60**, 2731 (1988).
[28] Z. Y. Ou, S. F. Pereira, H. J. Kimble, and K. C. Peng, Phys. Rev. Lett. **68**, 3663 (1992).
[29] J. C. Howell, R. S. Bennink, S. J. Bentley, and R. W. Boyd, Phys. Rev. Lett. **92**, 210403 (2004).
[30] J. S. Bell, Ann. N.Y. Acad. Sci. **480**, 263 (1986).
[31] E. P. Wigner, Phys. Rev. **40**, 749 (1932).
[32] L. M. Johansen, Phys. Lett. A **236**, 173 (1997).
[33] O. Cohen, Phys. Rev. A **56**, 3484 (1997).
[34] K. Banaszek and K. Wódkiewicz, Phys. Rev. A **58**, 4345 (1998).
[35] K. Banaszek and K. Wódkiewicz, Phys. Rev. Lett. **82**, 2009 (1999).
[36] Z.-B. Chen, J.-W. Pan, G. Hou, and Y.-D. Zhang, Phys. Rev. Lett. **88**, 040406 (2002).
[37] T. C. Ralph, W. J. Munro, and R. E. S. Polkinghorne, Phys. Rev. Lett. **85**, 2035 (2000).
[38] A. S. Parkins and H. J. Kimble, Phys. Rev. A **61**, 052104 (2000).
[39] H. Nha and H. J. Carmichael, Phys. Rev. Lett. **93**, 020401 (2004).
[40] M. Revzen, P. A. Mello, A. Mann, and L. M. Johansen, Phys. Rev. A **71**, 022103 (2005).
[41] P. H. S. Ribeiro, S. Pádua, J. C. Machado da Silva, and G. A. Barbosa, Phys. Rev. A **49**, 4176 (1994).
[42] P. H. S. Ribeiro, C. H. Monken, and G. A. Barbosa, Appl. Opt. **33**, 352 (1994).
[43] A. Joobeur, B. E. A. Saleh, T. S. Larchuk, and M. C. Teich, Phys. Rev. A **53**, 4360 (1996).
[44] G. A. Barbosa, Phys. Rev. A **54**, 4473 (1996).
[45] B. E. A. Saleh, A. Joobeur, and M. C. Teich, Phys. Rev. A **57**, 3991 (1998).
[46] B. E. A. Saleh, A. F. Abouraddy, A. V. Sergienko, and M. C. Teich, Phys. Rev. A **62**, 043816 (2000).
[47] A. F. Abouraddy, B. E. A. Saleh, A. V. Sergienko, and M. C. Teich, Phys. Rev. Lett. **87**, 123602 (2001).
[48] A. F. Abouraddy, B. E. A. Saleh, A. V. Sergienko, and M. C. Teich, J. Opt. Soc. Am. B **19**, 1174 (2002).
[49] R. S. Bennink, S. J. Bentley, R. W. Boyd, and J. C. Howell, Phys. Rev. Lett. **92**, 033601 (2004).
[50] I. F. Santos, L. Neves, G. Lima, C. H. Monken, and S. Pádua, Phys. Rev. A **72**, 033802 (2005).
[51] L. Neves, G. Lima, J. G. Arguirre Gómez, C. H. Monken, C. Saavedra, and S. Pádua, Phys. Rev. Lett. **94**, 100501 (2005).
[52] M. N. O'Sullivan-Hale, I. A. Khan, R. W. Boyd, and J. C. Howell, Phys. Rev. Lett. **94**, 220501 (2005).
[53] C. K. Hong, Z. Y. Ou, and L. Mandel, Phys. Rev. Lett. **59**, 2044 (1987).
[54] M. Atatüre, G. Di Giuseppe, M. D. Shaw, A. V. Sergienko, B. E. A. Saleh, and M. C. Teich, Phys. Rev. A **65**, 023808 (2002).
[55] G. Di Giuseppe, M. Atatüre, M. D. Shaw, A. V. Sergienko, B. E. A. Saleh, and M. C. Teich, Phys. Rev. A **66**, 013801 (2002).

[56] M. Atatüre, G. Di Giuseppe, M. D. Shaw, A. V. Sergienko, B. E. A. Saleh, and M. C. Teich, Phys. Rev. A **66**, 023822 (2002).
[57] S. P. Walborn, A. N. de Oliveira, S. Pádua, and C. H. Monken, Phys. Rev. Lett. **90**, 143601 (2003).
[58] S. P. Walborn, A. N. de Oliveira, R. S. Thebaldi, and C. H. Monken, Phys. Rev. A **69**, 023811 (2004).
[59] W. A. T. Nogueira, S. P. Walborn, S. Pádua, and C. H. Monken, Phys. Rev. Lett. **92**, 043602 (2004).
[60] S. P. Walborn, S. Pádua, and C. H. Monken, Phys. Rev. A **71**, 053812 (2005).
[61] S. Carrasco, J. P. Torres, L. Torner, A. Sergienko, B. E. A. Saleh, and M. C. Teich, Phys. Rev. A **70**, 043817 (2004).
[62] S. Carrasco, A. V. Sergienko, B. E. A. Saleh, M. C. Teich, J. P. Torres, and L. Torner, Phys. Rev. A **73**, 063802 (2006).
[63] Č. Brukner, M. S. Kim, J.-W. Pan, and A. Zeilinger, Phys. Rev. A **68**, 062105 (2003).
[64] A. G. White, D. F. V. James, P. H. Eberhard, and P. G. Kwiat, Phys. Rev. Lett. **83**, 3103 (1999).
[65] D. F. V. James, P. G. Kwiat, W. J. Munro, and A. G. White, Phys. Rev. A **64**, 052312 (2001).
[66] A. F. Abouraddy, A. V. Sergienko, B. E. A. Saleh, and M. C. Teich, Opt. Commun. **201**, 93 (2002).
[67] A. G. White, D. F. V. James, W. J. Munro, and P. G. Kwiat, Phys. Rev. A **65**, 012301 (2002).
[68] D. Porter and D. S. G. Stirling, *Integral Equations* (Cambridge University Press, Cambridge, 1990).
[69] S. Parker, S. Bose, and M. B. Plenio, Phys. Rev. A **61**, 032305 (2000).
[70] C. K. Law, I. A. Walmsley, and J. H. Eberly, Phys. Rev. Lett. **84**, 5304 (2000).
[71] C. K. Law and J. H. Eberly, Phys. Rev. Lett. **92**, 127903 (2004).
[72] S. Hill and W. K. Wootters, Phys. Rev. Lett. **78**, 5022 (1997).
[73] W. K. Wootters, Phys. Rev. Lett. **80**, 2245 (1998).
[74] A. F. Abouraddy, B. E. A. Saleh, A. V. Sergienko, and M. C. Teich, Phys. Rev. A **64**, 050101(R) (2001).
[75] J. T. Barreiro, N. K. Langford, N. A. Peters, and P. G. Kwiat, Phys. Rev. Lett. **95**, 260501 (2005).
[76] D. N. Klyshko, Zh. Eksp. Teor. Fiz. Pis'ma Red. **6**, 490 (1967) [JETP Lett. **6**, 23 (1967)].
[77] T. G. Giallorenzi and C. L. Tang, Phys. Rev. **166**, 225 (1968).
[78] D. A. Kleinman, Phys. Rev. **174**, 1027 (1968).
[79] C. K. Hong and L. Mandel, Phys. Rev. A **31**, 2409 (1985).